

Supporting information

Investigations of the structural evolution of electrospun nanofibers using atomic force microscopy

Peng Xu ^{a,b}, Wei Li ^{a,c,*}, Huacong Zhou ^{a,b}, Huifang Xing ^a, Feng Pan ^a, Huizhou Liu ^{a,*}

^a *State Key Laboratory of Biochemical Engineering,*

Key Laboratory of Green Process and Engineering,

Institute of Process Engineering, Chinese Academy of Sciences, Beijing 100190, China

^b *Graduate School of Chinese Academy of Science, Beijing 100039, China*

^c *Department of chemistry, Capital Normal University, Beijing, 100048, China*

*Corresponding author, Tel: +86-10-62554254, Fax: +86-10-62554264, e-mail addresses:

wli@cnu.ac.edu.cn (W. Li), hzliu@home.ipe.ac.cn (H. Liu).

SI1. FT-IR Analysis

FT-IR analysis was provided to further elucidate the incorporation of BSA in nanofibers. Fig. S1 showed the FT-IR spectra of PEO, BSA, chitosan, nanofibers with/without BSA. All the stretching and bending vibrations matched well with the theoretical values. For nanofibers without BSA (curve S1d), the sharp peak at 1360 cm^{-1} and 1061 cm^{-1} were attributed to the $-\text{CH}_2$ symmetric wagging and the $-\text{COC}-$ asymmetric stretching mode coupled with the $-\text{CH}_2$ symmetric rocking mode of PEO, respectively ¹. The broad band of PEO attributed to the stretching vibration of $-\text{OH}$ moved from 3454 cm^{-1} (curve S1a) ¹ to 3416 cm^{-1} (curve S1d) due to the formation of hydrogen bonds. Besides, a new peak at 1561 cm^{-1} in curve S1d was attributed to the asymmetric stretching of $-\text{NH}_3^+$, because chitosan formed ammonium salts when $\text{pH} < 6$ (the pH of solution was about 3.5) ². Fig. S1d and S1e were then picked out and shown in Fig. S2. Obviously, as shown in Fig. S2, the intensity of amide regions

(amide I at 1654 cm^{-1} and amide II at 1546 cm^{-1}) of fibers without BSA was much weaker than the peak intensity of C-O stretching at 1080 cm^{-1} , while in the case of fibers with BSA, the peak intensity of amide I (1654 cm^{-1}) and amide II (1541 cm^{-1}) increased sharply, which was clearly a signal of the incorporation of BSA.

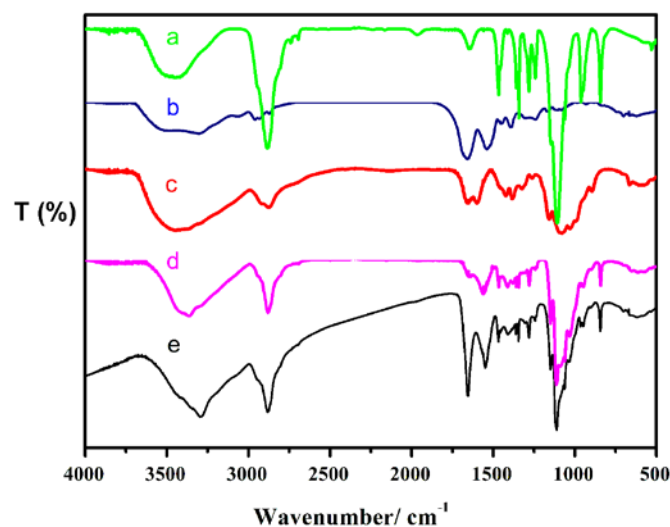


Figure S1. FT-IR spectra of pure PEO (a), native BSA (b), chitosan ($M_w=560\text{ kDa}$) (c), nanofibers mat without BSA (d) and with BSA (e).

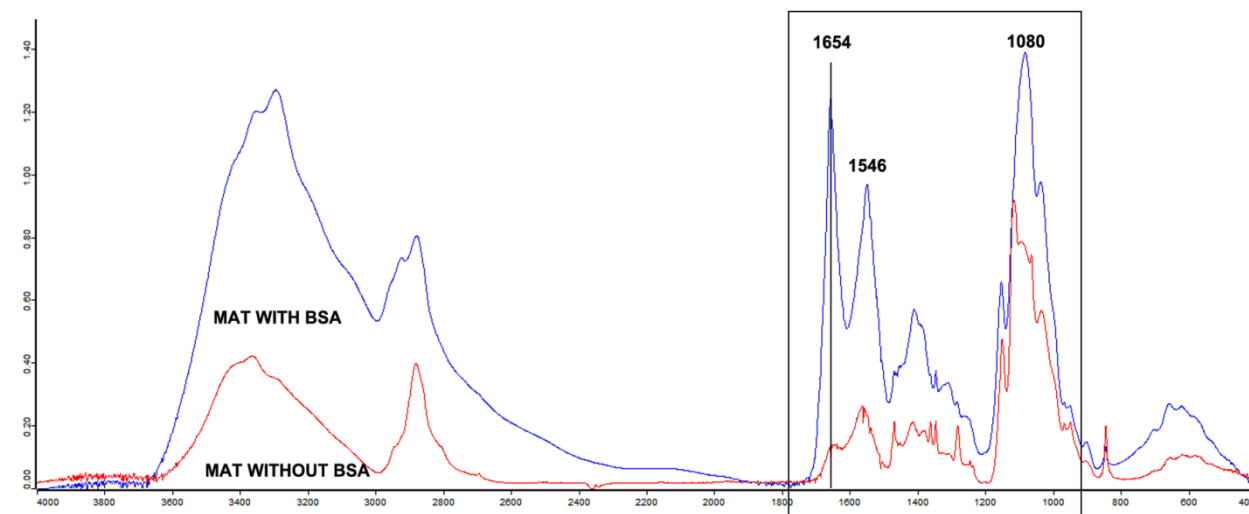


Fig. S2. FT-IR spectra of electrospun fibers without BSA (red curve) and with BSA (blue curve).

Compared with curve S1d (nanofibers without BSA), the broad band at 1654 cm^{-1} of α -helix BSA³ became sharp and peaks belonged to β -sheet and turns in curve S1b of native BSA were not observed in curve S1e (nanofibers with BSA). As we know, when the pH of polymer solution is below the isoelectric point of BSA ($\text{pI}=4.8$), $-\text{NH}_2$ group of BSA will get positive charges. Hence, we speculated that the increasing charge repulsion restrained the formation of hydrogen bonds of β -sheet and turns of BSA in curve S1e. On the other hand, the broad peak at 3363 cm^{-1} (curve S1d), which was attributed to the stretching vibration of $-\text{NH}_2$ coupled with $-\text{OH}$, moved to 3291 cm^{-1} (curve S1e), because more hydrogen bonds formed by adding BSA. Compared the spectra of nanofibers with/without BSA, no new chemical bonds formed expect some peaks shift. It implied that the probable way of immobilizing BSA was only mechanical mixing accompanied with some hydrogen bonds formation without changing its chemical structures.

In electrospinning, many parameters such as voltage, distance between collector and nozzle can influence the formation process, which have been extensively investigated⁴⁻⁷. Our work concentrated on the influence of the solution properties: weight ratios of polymers and molecular weights (M_w) of chitosan. The investigations of the two parameters gave more details about the formation of nanofibers.

SI2. Effects of different weight ratios of chitosan: PEO

Five weight ratios of chitosan: PEO (33:67, 50:50, 60:40, 75:25 and 80:20) were selected to study their effects on electrospinning process. Process of fibers with different weight ratios were shown in Fig. S3.

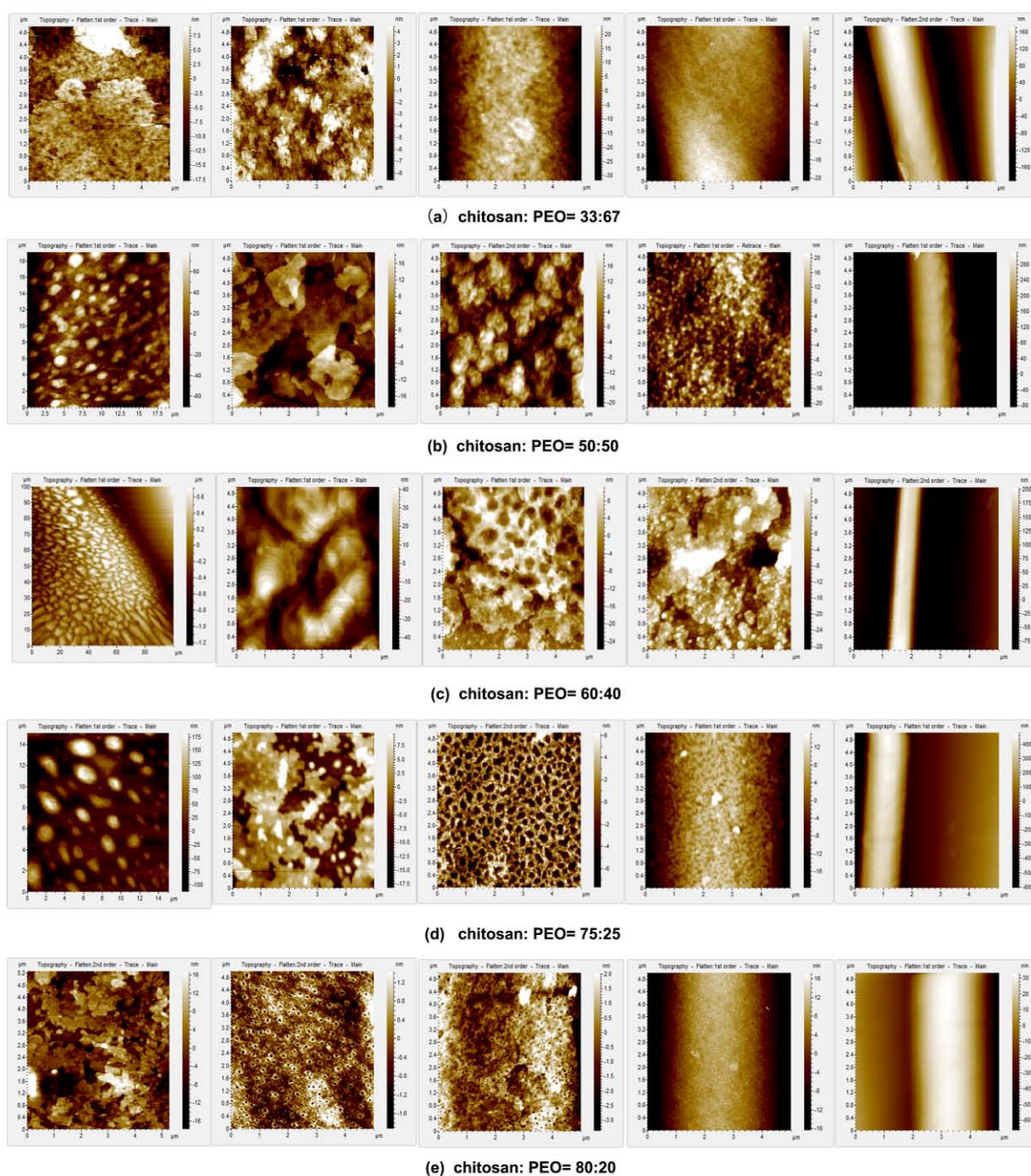


Figure S3. AFM topographies of jets with different chitosan:PEO weight ratios: 33:67 (a), 50:50 (b), 60:40 (c), 75:25 (d) and 80:20 (e), respectively.

It was found that the structural evolution of fibers varied greatly with different weight ratios of chitosan: PEO (summarized in Table S1). As listed in Table S1, features of plates, bumps and smoothness appeared in all the process of different

weight ratios. However, the stage of columns didn't show up when weight ratios were 33:67 and 80:20. In addition, it was not until the weight ratio was increased to 60:40 that micropores appeared.

Table S1. Characteristic structures of jets with different weight ratios of chitosan:PEO

Features Weight ratio	Columns	Plates	Micropores	Bumps	Smoothness
33:67 (Fig. S3a)	x	✓	x	✓	✓
50:50 (Fig. S3b)	✓	✓	x	✓	✓
60:40 (Fig. S3c)	✓	✓	✓	✓	✓
75:25 (Fig. S3d)	✓	✓	✓	✓	✓
80:20 (Fig. S3b)	x	✓	✓	✓	✓

There were two reasons contributed to the results. Firstly, as presented in Fig. S4, the viscosity and conductivity of solution changed with different weight ratios of chitosan: PEO. The viscosity increased from 6000 to 28000 mPa·s when the weight ratio increased from 33:67 to 80:20. Conductivity had the same tendency with viscosity, but it did not vary as much. Thus increasing the proportion of chitosan primarily increased the viscosity of solution, which made the solution more unspinnable⁸. Fiber with weight ratio of 33:67 (~6000 mPa·s, the lowest viscosity) transformed too fast to maintain columns after it was emitted from the apex. On the contrary, high viscosity not only made it difficult to elongate jets, but also restricted fluctuations (lead to columns) in electric field, since more force was required to overcome the surface tension. Maybe it was the reason why columns were not formed when the weight ratio was changed to 80:20 (27654 mPa·s, the highest viscosity). Secondly, it had been reported that the glass transition temperature (T_g) played a critical role in the formation of porous structures, i.e., polymers with low T_g were

more difficult to form micropores than the polymers with high T_g ⁹. In our work, the T_g of PEO was very low (-67 °C), while the T_g of chitosan was about 145 °C¹⁰. So the proportion of the two polymers influenced pores formation, that is, when the content of chitosan in solution was low, the low T_g would resist micropores' formation (Fig. S3a and S3b).

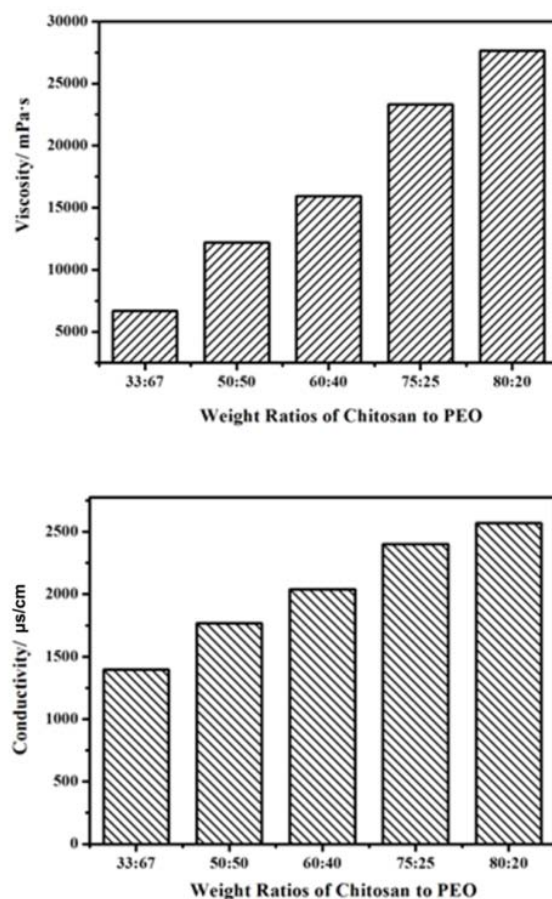
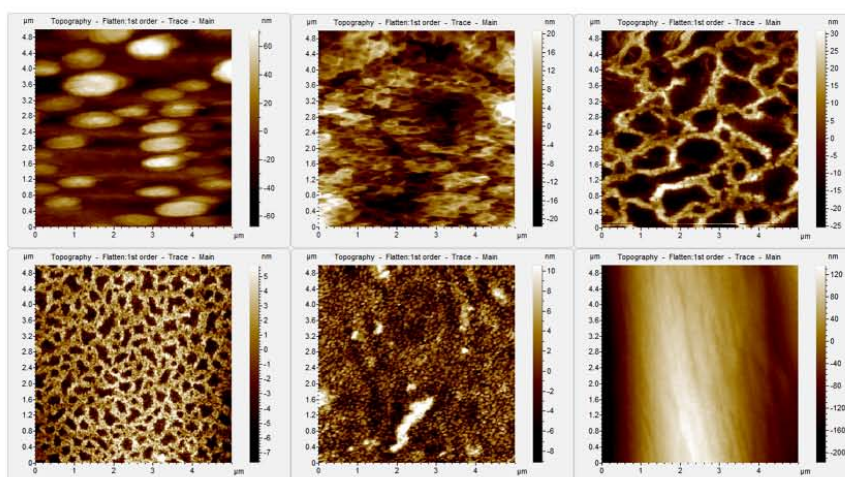


Figure S4. Effects of different weight ratios of chitosan: PEO on solution viscosity and conductivity.

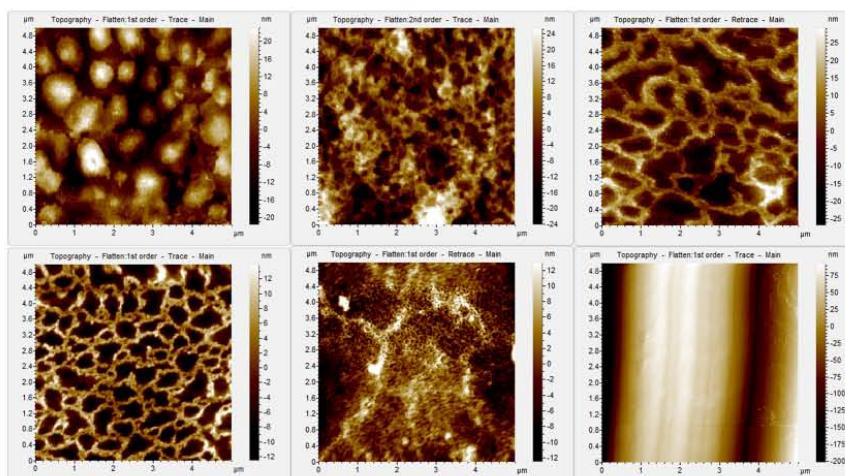
SI3. Effects of M_w of chitosan on fiber's formation

To investigate the influences of different M_w on fiber's formation, chitosan with three M_w of 100 kDa, 200 kDa and 560 kDa were employed in the work. The experiments were conducted with the same weight ratio of chitosan: PEO (60:40), and the other parameters were also same (flow rate of the solution was 3 mL/h, voltage

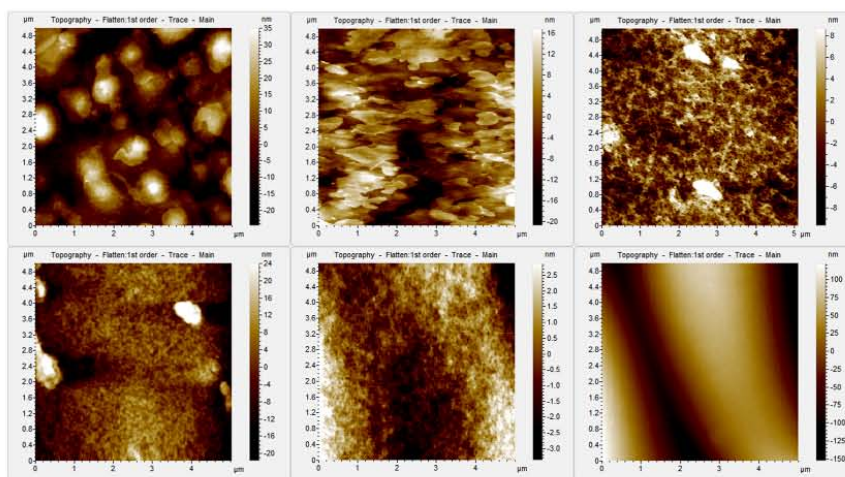
was 17 kV and the tip-to-collector distance was 14 cm). Fig. S5 (a), (b), and (c) showed the process of jet with different chitosan M_w of 100 kDa, 200 kDa, and 560 kDa, respectively. Considering the main process was similar, more details of surface evolution were given. Taken together, the five stages in the process were unchanged with different M_w of chitosan, except a few alterations. We could see that the jet surface structures of 560 kDa (Fig. S5c) didn't change dramatically as others (100 kDa, Fig. S5a and 200 kDa, Fig. S5b) — the columns didn't totally extrude out and micropores were shallower and smaller. It could be explained by the different properties of solutions



(a)



(b)



(c)

Figure S5. Structural evolution of jets with different M_w of chitosan in electrospinning: 100 kDa (a), 200 kDa (b), and 560 kDa (c), respectively.

Fig. S6 was the characteristic variations of different solution. The viscosity increased rapidly while the conductivity changed little with increasing the M_w of chitosan. So we deduced that the viscosity was the main factor influencing the process. High viscosity made it more difficult to form microstructures on surface. At the same time, the relaxation of polymer chains became more difficult with increasing the M_w of chitosan, which prevented the jet from having significant structural changes during the evolution¹¹.

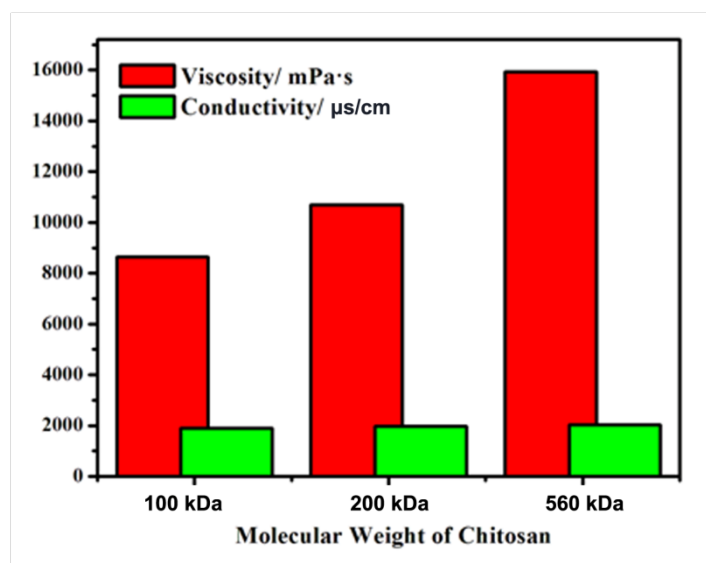


Figure S6. Effects of different M_w of chitosan on solution viscosity and conductivity.

References

1. Y. Fang, X. Zhu, D. Yan, Q. Lu and P. Zhu, *Colloid and Polymer Science*, 2002, **280**, 59-64.
2. C. K. S. Pillai, W. Paul and C. P. Sharma, *Prog Polym Sci*, 2009, **34**, 641-678.
3. T. Maruyama, S. Katoh, M. Nakajima, H. Nabetani, T. P. Abbott, A. Shono and K. Satoh, *Journal of Membrane Science*, 2001, **192**, 201-207.
4. J. M. Deitzel, J. Kleinmeyer, D. Harris and N. C. Beck Tan, *Polymer*, 2001, **42**, 261-272.
5. S. H. Tan, R. Inai, M. Kotaki and S. Ramakrishna, *Polymer*, 2005, **46**, 6128-6134.
6. S. A. Theron, E. Zussman and A. L. Yarin, *Polymer*, 2004, **45**, 2017-2030.
7. T. Uyar and F. Besenbacher, *Polymer*, 2008, **49**, 5336-5343.
8. B. M. Min, S. W. Lee, J. N. Lim, Y. You, T. S. Lee, P. H. Kang and W. H. Park, *Polymer*, 2004, **45**, 7137-7142.
9. Z. Q. Lin, T. Kerle, T. P. Russell, E. Schaffer and U. Steiner, *Macromolecules*, 2002, **35**, 3971-3976.
10. Y. M. Dong, Y. H. Ruan, H. W. Wang, Y. G. Zhao and D. X. Bi, *Journal of Applied Polymer Science*, 2004, **93**, 1553-1558.
11. A. Koski, K. Yim and S. Shivkumar, *Mater Lett*, 2004, **58**, 493-497.